# Description of Gloeomargarita ahousahtiae sp. nov. (Gloeomargaritales), a thermophilic cyanobacterium with intracellular carbonate inclusions

Thomas Bacchetta, Purificación López-García, Ana Gutiérrez-Preciado, Neha Mehta, Feriel Skouri-Panet, Karim Benzerara, Maria Ciobanu, Naoji Yubuki, Rosaluz Tavera, David Moreira

# Description of *Gloeomargarita ahousahtiae* sp. nov. (Gloeomargaritales), a thermophilic cyanobacterium with intracellular carbonate inclusions

Thomas Bacchetta[a], Purificación López-García[a], Ana Gutiérrez-Preciado[a], Neha Mehta[b], Feriel Skouri-Panet[b], Karim Benzerara[b], Maria Ciobanu[a], Naoji Yubuki[a,c], Rosaluz Tavera[d] and David Moreira[a]

[a] Unité d'Ecologie Systématique et Evolution, CNRS, Université Paris-Saclay, AgroParisTech, Gif sur Yvette 91190, France; [b] Institut de Minéralogie, de Physique des Matériaux et de Cosmochimie (IMPMC), Sorbonne Université, Muséum National d'Histoire Naturelle, UMR CNRS 7590, Paris 75005, France; [c]UBC Bioimaging Facility, University of British Columbia, Vancouver, BC V6T 1Z4, Canada; [d]Departamento de Ecología y Recursos Naturales, Universidad Nacional Autónoma de México, DF Mexico 04510, Mexico

**ABSTRACT**

A unicellular cyanobacterium, strain VI4D9, was isolated from thermophilic microbial mats thriving in a hot spring of the Ahousaht territory of Vancouver Island, Canada, and characterized using optical and electron microscopy, genome sequencing and cultivation approaches. The cells were elongated rods (5.1 μm in length and 1.2 μm in width, on average). Their UV visible absorption spectra revealed that they contain chlorophyll *a*, phycocyanin and carotenoids. Transmission electron microscopy showed the presence of thylakoids concentrated on one side of the cells. The strain grew within a temperature range of 37–50°C, with an optimum growth at 45°C. Its genome had a size of 3 049 282 bp and a DNA G + C content of 51.8 mol%. The cells contained numerous intracellular spherical granules easily visible under scanning electron microscopy. Energy dispersive X-ray spectroscopy revealed that these granules were made of Ca-, Ba- and Sr-containing carbonates. A phylogenetic 16S rRNA gene tree robustly placed this strain as sister to several environmental sequences and the described species *Gloeomargarita lithophora*, also characterized by the possession of intracellular carbonate inclusions. We consider strain VI4D9 to represent a new *Gloeomargarita* species based on its marked phenotypic differences with *G. lithophora*, notably, its thermophilic nature and different thylakoid organization, therefore we propose the name *Gloeomargarita ahousahtiae* sp. nov. The type strain is VI4D9 (Culture Collection of Algae and Protozoa strain 1472/1; Laboratorio de Algas Continentales Mexico strain LAC 140). *Gloeomargarita ahousahtiae* is the second species described within the recently discovered order Gloeomargaritales.

**HIGHLIGHTS**

- *Gloeomargarita ahousahtiae* is a new thermophilic cyanobacterium.
- Growth temperature and thylakoid morphology differentiate *G. ahousahtiae* and *G. lithophora*.
- All described Gloeomargaritales synthesize intracellular carbonate inclusions.

**KEYWORDS** Blue-green algae; chlorophyll *a*; cyanobacteria; fresh water; genome sequencing; Gloeomargaritales; intracellular biomineralization; microbial mats; new species; thermophilic cyanobacteria

## Introduction

The first photosynthetic eukaryotes to evolve, the Archaeplastida (including red algae, glaucophytes and land plants plus green algae), emerged through a symbiosis that involved a cyanobacterial endosymbiont and a heterotrophic eukaryotic host (Moreira & Philippe, 2001; Keeling, 2013). This oxygenic photosynthetic capability was later transferred to other eukaryotic lineages through secondary and tertiary endosymbioses involving green and red algae as endosymbionts (McFadden, 2001; Keeling, 2013; Ponce-Toledo *et al.*, 2019). The monophyly of Archaeplastida has been found in phylogenetic trees reconstructed both with plastid- and nucleus-encoded markers (Moreira *et al.*, 2000; Rodríguez-Ezpeleta *et al.*, 2005; Irisarri *et al.*, 2021), hence supporting the hypothesis that a single primary endosymbiosis gave rise to this group. However, the identity and lifestyle of the cyanobacterial endosymbiont involved in this major evolutionary event have long been debated.

Different studies have alternatively proposed early- and late-branching cyanobacteria (e.g. Blank, 2013; Dagan *et al.*, 2013) but the cyanobacterial sister group of plastids has only recently been confidently identified. This group is represented by the deep-branching cyanobacterium *Gloeomargarita lithophora* strain Alchichica- D10 (Ponce-Toledo *et al.*, 2017), which was isolated from microbialite samples from Lake Alchichica in Mexico (Couradeau *et al.*, 2012; Moreira *et al.*, 2018). Phylogenetic analysis of conserved protein markers supported that *G. lithophora* defined a new

cyanobacterial order, the Gloeomargaritales (Moreira *et al*., 2018). *G. lithophora* exhibits the unusual ability to synthesize large amounts of intracellular amorphous calcium (Ca) carbonate inclusions, sometimes enriched in barium and strontium (Couradeau *et al*., 2012; Benzerara *et al*., 2014). While cyanobacteria have been known for long to induce extracellular Ca carbonate precipitation as a consequence of the environmental pH increase triggered by photosynthesis (Riding, 2006), this intracellular biomineralization process was only recently discovered in several cyanobacterial lineages (Cam *et al*., 2017; Benzerara *et al*., 2022). Moreover, *G. lithophora* has a unique preference to incorporate barium (Ba), followed by strontium (Sr) and lastly Ca within the intracellular carbonate inclusions (Cam *et al*., 2016; Mehta *et al*., 2022).

Up to now, *G. lithophora* was the only isolated species within the Gloeomargaritales. Nevertheless, environmental surveys identified a large diversity of related 16S rDNA sequences in diverse freshwater environments, mostly microbialites and thermophilic microbial mats (Ragon *et al*., 2014). Moreover, *Gloeomargarita*- like cells containing intracellular carbonates have also been observed by electron microscopy in microbial mat samples of the Meskoutine hot spring in Algeria (Amarouche-Yala *et al*., 2014), although they have never been grown in the laboratory. Here, we describe the second isolated Gloeomargaritales strain: *Gloeomargarita ahousahtiae* strain VI4D9, the first thermophilic species of this genus, also capable of synthesizing intracellular carbonate inclusions.

## Materials and methods

### *Sampling site and isolation*

Thermophilic microbial mat samples were collected in sterile plastic containers in August 2005 in Hot Springs Cove (49°30′59.69″N, 126°15′36.33″W; Vancouver Island, Canada) and transported to the laboratory at room temperature. Physicochemical parameters were measured *in situ* with a YSI Professional Series Plus multiparameter probe. Since that sampling date, the mats were maintained in laboratory aquaria (Supplementary fig. S1) in their habitat water at 45°C under a 12 h–12 h light-dark cycle with light intensity of 10 μmol photons $m^{-2}s^{-1}$.

To isolate new non-filamentous cyanobacterial species from the biofilms growing in these aquaria, the biofilm cells were initially resuspended in distilled water by vortexing and repeated pipetting, and subsequentlythe cell suspension was filtered through a 5 μm pore size filter. Filtrate volumes ranging from 0.5–2 μl were then used to inoculate three 96- well microplates containing BG-11 medium (Stanier *et al*., 1971). Microplates were incubated at 45°C for 2 months under a dark-light (12 h–12 h) cycle. Wells with cyanobacterial growth (identified by their blue-green colouration) were serially diluted in BG-11 until pure cultures were obtained.

Cultures did not grow under agitation. Therefore, growth rate was estimated as the time that the cultures required to cover the bottom of the culture flasks starting from identical inoculum amounts. To determine optimum growth temperature, cultures were incubated at temperatures between 20°C and 60°C, at steps of 5°C. Possible incorporation of Ba and Sr was tested by growth in BG-11 supplemented with these elements at a final concentration of 25 μM.

### *Optical and electron microscopy*

Phase contrast and differential interference contrast (DIC) microscopy observations were done using a Zeiss Axioplan 2 Imaging light microscope (Jena, Thuringia, Germany). Pictures were taken with both an AxiocamMR camera using the Zeiss AxioVision 4.8.2 SP1 suite and a Sony α9 (Minato, Tokyo, Japan) digital camera. These images were used to measure the cell dimensions on 62 cells.

Two different scanning electron microscope (SEM) techniques were applied in order to detect the possible presence of intracellular polyphosphate and carbonate inclusions. In one, dehydrated cells were observed that had previously been filtered on 0.22 μm polyethersulfone (PES) filters, rinsed with Milli-Q water and dried at ambient temperature. These cell-covered PES filters were mounted on aluminium stubs using double- sided carbon tape and carbon-coated prior to SEM observation with a Zeiss Ultra55 SEM microscope (Jena, Thuringia, Germany). In the other, fresh non- dehydrated cells were deposited on 0.22 μm PES filters and observed using a Hitachi SU5000 FEG Low Vacuum microscope (Tokyo, Japan).

The chemical composition of intracellular carbonate inclusions was studied using scanning transmission electron microscopy (STEM) and an energy dispersive x-ray spectrometer (EDXS). STEM analyses were performed in the high-angle annular dark-field (HAADF) mode using a JEOL 2100 F microscope (Akishima, Tokyo, Japan) operating at 200 kV and equipped with a field emission gun and a JEOL EDXS detector. For STEM observations, cyanobacterial cells were harvested by centrifugation at 10 000 g (5 min) and the cell pellets were washed twice before resuspension in 500 μl of Milli-Q water and deposited on pre-ionized carbon- coated 200-mesh copper grids.

Ultrathin sections were prepared for transmission electron microscopy (TEM) in order to study the presence of intracellular structures such as thylakoids and carboxysomes. Cells were collected by centrifugation (10 000 g, 5 min) and resuspended in a solution of 2.5% glutaraldehyde and 2%

paraformaldehyde in 0.2 M sodium cacodylate buffer (pH 7.2) (Karnovsky,
1964). After rinsing the cells with the buffer, the suspension was fixed in 1% osmium tetroxide, followed by dehydration through an ethanol bath series of 10 min each at concentrations of 30%, 50%, 70%, 90%, followed by 3 baths of 10 min in 100% ethanol before final substitution with acetone (Hayat, 2000). The fixed cells were embedded in Agar low viscosity resin (Agar Scientific) and thin sections were prepared with a diamond knife mounted on a Leica UC6 ultramicrotome (Wetzlar, Germany) and observed with a JEOL JEM 1400 microscope
(Akishima, Tokyo, Japan).

### *Pigment characterization*

Cells were collected by centrifugation (10 000 g, 5 min) of a 5 ml culture and pigments were purified from the cell pellet by 100% acetone overnight extraction at 4°C. The absorption spectrum of different dilutions of the pigments was measured with a Hach DR 5000 spectrophotometer (Ontario, Canada) in the wavelength range from 350–800 nm.

### *DNA extraction, 16S rRNA gene amplification and phylogenetic analysis, and genome sequencing*

Cyanobacterial cells were collected by centrifugation of liquid cultures at 10 000 g for 5 min and DNA was extracted from cell pellets with the DNeasy PowerBiofilm kit (Qiagen) following manufacturer's instructions.

16S rRNA genes were amplified by PCR using the two Gloeomargaritales-specific primers 69 F-Gloeo (AAGTCGAACGGGGKWGCAA) and 1227 R-Gloeo (GATCTGAACTGAGACCAAC), which produced amplicons of ~1200 bp (Ragon *et al*., 2014). PCR reactions were done in 25 µl of reaction buffer, containing 1 µl of the eluted DNA, 1.5 mM $MgCl_2$, dNTPs (10 nmol each), 20 pmol of each primer, and 0.2 U Taq platinum DNA polymerase (Invitrogen). PCR reactions were run under the following conditions: 35 cycles (denaturation at 94°C for 15s, annealing at 55°C for 30s, extension at 72°C for 2 min) preceded by a 2-min denaturation step at 94°C, and followed by a 7-min extension step at 72°C. Positive amplicons were sequenced using the Sanger sequencing method with the same amplification primers (Beckman Coulter Genomics, Takeley, UK).

The new 16S rRNA gene sequence was included in a multiple sequence alignment containing a selection of cyanobacterial sequences (based on Ponce-Toledo *et al*., 2017) and enriched in Gloeomargaritales sequences identified using the new sequence as query in a BLAST search (Altschul *et al*., 1997) against the non-redundant (nr) GenBank database (http://www.ncbi.nlm.nih.gov/). Sequences were aligned using MAFFT (Katoh & Standley, 2013) with default parameters and poorly aligned regions were removed with trimAl –automated1 (Capella- Gutiérrez *et al*., 2009). The resulting alignment was used as input to build a maximum likelihood (ML) phylogenetic tree using IQ-TREE (Nguyen *et al*., 2015) with the general time reversible (GTR) model of sequence evolution, and taking among-site rate variation into account by using a four-category discrete approximation of a Γ distribution. ML bootstrap proportions were inferred using 1000 replicates. The tree was visualized with FigTree (http://tree.bio.ed.ac. uk/software/figtree/).

Genomic DNA was extracted from a liquid culture as explained above and sequenced using both short (2 × 125 bp paired-end Illumina HiSeq 2500) and long (2–10 kb Nanopore MinION) reads. A hybrid assembly of these short and long reads was produced with Unicycler v0.4.9b (Wick *et al*., 2017). The assembled genome was annotated with Prokka v1.14.5 (Seemann, 2014). To compare different genomes, we used average nucleotide identity (ANI), estimated using the EZBioCloud ANI Calculator (Yoon *et al*., 2017), and the digital DNA-DNA hybridization (dDDH), estimated using the GGDC calculator (Meier-Kolthoff *et al*., 2021).

## Results

### *Isolation of a new Gloeomargaritales cyanobacterium*

We collected samples of thermophilic microbial mats growing on a small, moderately hot (45–47°C), circumneutral (pH 7.5) and sulphur-rich stream in the Hot Springs Cove hydrothermal system (Supplementary fig. S2) in Vancouver Island (Canada). Using serial dilution and incubation at 45°C, we isolated a new cyanobacterial strain, VI4D9. Phylogenetic analysis of its 16S rRNA gene sequence showed that it was closely related to three environmental sequences obtained from various hot springs of the Yellowstone National Park (Fig. 1). This group of sequences from hydrothermal systems branched as sister to the group containing the only Gloeomargaritales species described so far, *Gloeomargarita lithophora*. We named the new strain VI4D9 *Gloeomargarita ahousahtiae* under the International Code of Nomenclature for algae, fungi and plants (McNeill *et al*., 2012; see the Taxonomic analysis below).

### *Phenotypic characteristics of* Gloeomargarita ahousahtiae

Cells grew mainly attached to surfaces and their growth was faster in glass culture flasks than in plastic flasks. Since this strain had a benthic lifestyle and agitation to obtain cultures in suspension was deleterious at all temperatures, no measurement of growth rate and generation time based on culture optical density was possible. Growth was therefore measured as the time that the strain required to cover the bottom of the culture flasks. We examined the growth of the new strain in BG-11 medium at different temperatures ranging from 20–60°C. Growth was detected only at temperatures between 37°C and 50°C, with an optimum at 45°C.

*Gloeomargarita ahousahtiae* cells were short rods that measured 5.1 ± 0.9 µm in length and 1.2 ± 0.02 µm in width (from 62 cells measured) (Figs 2, 3) and divided by binary fission. These cells were longer than those of *G. lithophora* (3.9 ± 0.6 µm in length and 1.1 ± 0.1 µm in width) (Moreira *et al.*, 2018). The cultures were intensely coloured (Fig. 4). The absorption spectrum of acetone-extracted *G. ahousahtiae* pigments showed two absorption peaks at 437 and 662 nm typical of chlorophyll *a*, a peak at 616 nm likely corresponding to phycocyanin, and a typical carotenoid peak at 478 nm (Figs 5, 6). This pigment combination is characteristic for the majority of freshwater cyanobacteria (Chen *et al.*, 2021).

Using scanning electron microscopy (SEM), we noticed that *G. ahousahtiae* forms intracellular amorphous carbonate inclusions scattered within the cytoplasm, albeit often arranged in a rather linear configuration (Figs 7, 8). These carbonate inclusions were accompanied by polyphosphate granules, clearly recognizable by their lower brightness under SEM observation (Figs 8, 9). The cells also contained icosahedral structures probably corresponding to

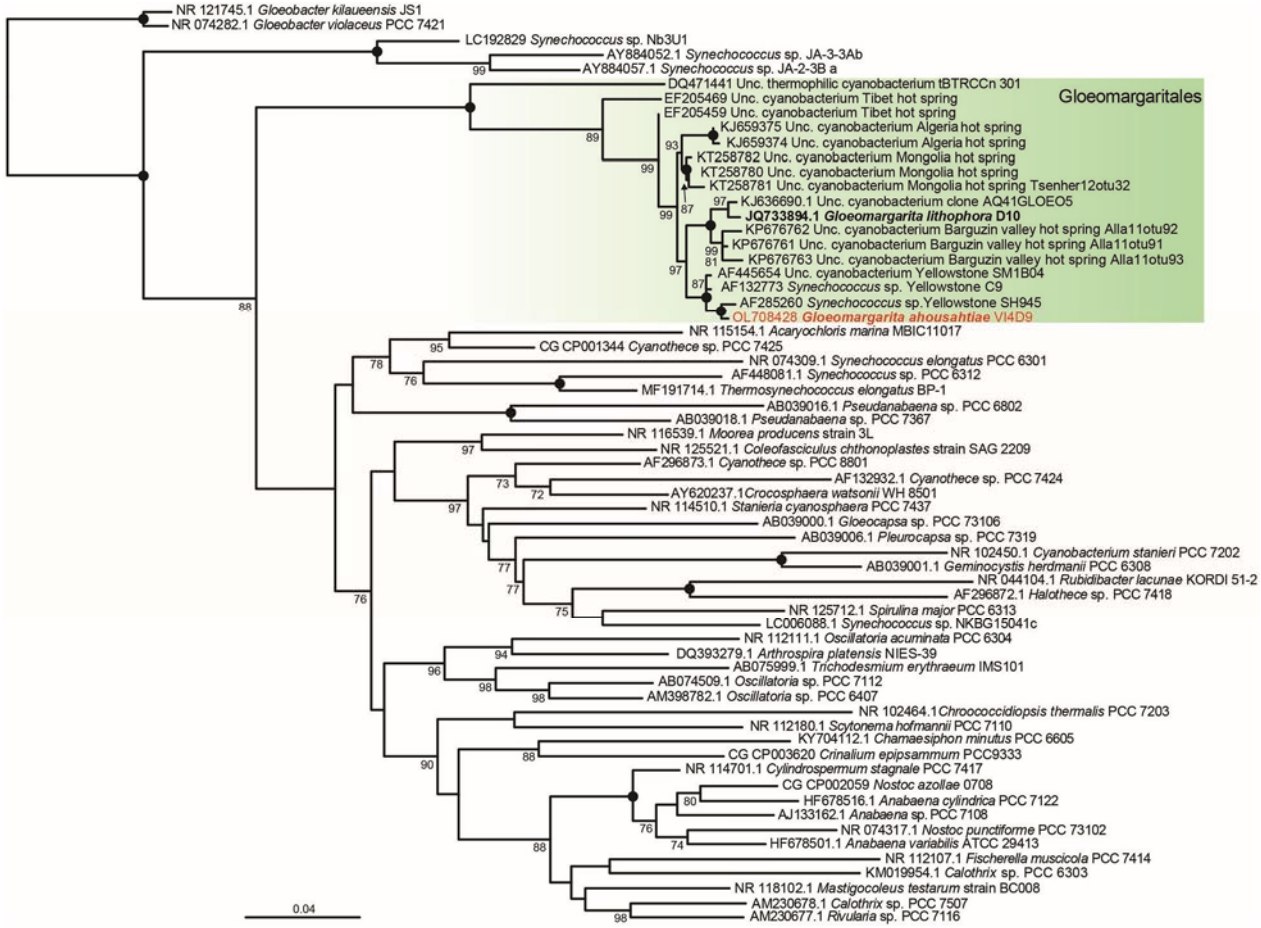


**Fig. 1.** 16S rRNA gene maximum likelihood phylogenetic tree of cyanobacteria showing the position of *Gloeomargarita ahousahtiae* within the Gloeomargaritales (green clade). Numbers on branches are bootstrap proportions (only values > 70% are shown); black circles indicate 100% bootstrap values.

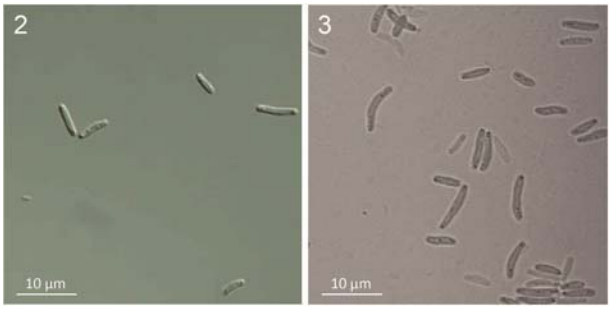


**Figs 2, 3.** Optical microscopy images of *Gloeomargarita ahousahtiae*. **Fig. 2**. Differential interference contrast image. **Fig. 3**. Phase contrast image.

carboxysomes (Fig. 8). Inspection of the cell surface at high magnification showed a finely dotted pattern (Fig. 10).

To test whether *G. ahousahtiae* also had the ability to selectively uptake Ba and Sr into the intracellular carbonate inclusions (Cam *et al.*, 2016), we incubated our strain in BG-11 medium amended with these elements. After one month of growth, the composition of intracellular carbonate inclusions was analysed. The detection of characteristic peaks of Ba, Sr and Ca in the SEM-EDXS spectrum provided the first clue that *G. ahousahtiae* accumulated all these elements within the intracellular inclusions (Fig. 11). Furthermore, STEM-HAADF revealed that some intracellular inclusions had a brighter core surrounded by a darker layer, whereas other inclusions exhibited uniform high brightness (Fig. 12). The EDXS analysis showed that inclusions made only of Ba, Sr or Ca were those that appeared as uniform bright spheres in the STEM-HAADF observations, whereas inclusions that had a Ba or Sr core surrounded by a layer of Sr or Ca were those that showed the differential layered brightness (Figs 13–17). Based on a comparison with what was previously observed for *G. lithophora* (Cam *et al.*, 2016), the formation of these layered intracellular carbonates suggested that *G. ahousahtiae* selectively uptakes Ba and Sr over Ca. The cells also contained phosphorus-rich inclusions that were most likely polyphosphate bodies (Fig. 17).

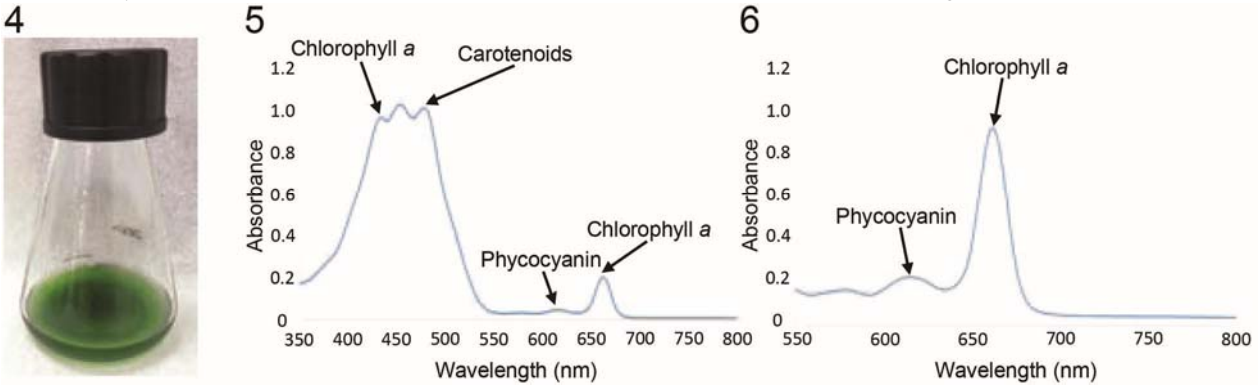


**Figs 4–6.** Pigments of *Gloeomargarita ahousahtiae*. **Fig. 4**. View of a liquid culture after one month of growth, showing a typical cyanobacterial colour. **Fig. 5**. Absorbance spectrum (between 350–800 nm) of *G. ahousahtiae* pigments purified by 100% acetone extraction. **Fig. 6**. Absorbance spectrum (between 550–800 nm) of *G. ahousahtiae* concentrated (4×) pigments to better appreciate the phycocyanin peak.

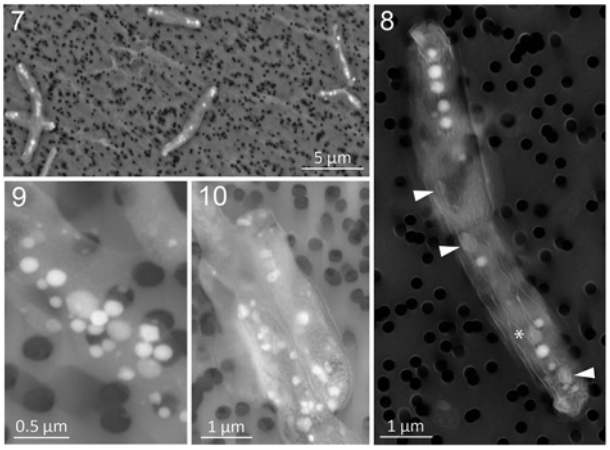


**Figs 7–10.** Scanning electron microscopy images of *Gloeomargarita ahousahtiae* cells. **Fig. 7**. General view of several fresh cells observed under low vacuum; notice the bright intracellular carbonate inclusions. **Fig. 8**. Image of a dried cell acquired using the secondary electron (SE) mode. In addition to bright carbonate inclusions, the cell also contains a few darker, and generally bigger, polyphosphate granules (white arrowheads), as well as carboxysomes (white asterisk). **Fig. 9**. Close view of bright (carbonate) and grey (polyphosphate) inclusions in a fresh cell observed under low vacuum with a BSE detector. **Fig. 10**. Overlay of images of fresh cells acquired using backscattered (BSE) and secondary (SE) electron detectors under low vacuum; notice the finely dotted cell surface.

Transmission electron microscopy (TEM) observation of thin sections (n = 20) showed that *G. ahousahtiae* cells exhibited a typical Gram-negative structure with two membranes and a thin intermediate peptidoglycan wall (Figs 18, 19). In contrast with the concentric thylakoids close to the cell membrane found in *G. lithophora* (Moreira *et al.*, 2018), those of *G. ahousahtiae* were mainly located along one side of the cell (Fig. 18). Many structures with low electron density were observed in the cytoplasm (Fig. 20).

### *Genome characteristics and comparison with* G. lithophora

The complete genome sequence of *G. ahousahtiae* had a length of 3 162 419 bp, a G + C content of 51.8 mol%, and encoded 3141 genes, including 3059 protein-coding genes. A single rRNA locus was present, as well as genes for all common tRNAs. 1495 (48.9%) of the protein-coding genes were annotated in comparison with proteins with known biological functions and 1564 (51.1%) remained annotated as hypothetical. These general values were similar to those of the *G. lithophora* genome, which has a size of 3 049 282 bp, a G + C content of 52.2 mol%, and encodes 3101 genes

(Moreira *et al*., 2018). 2463 genes of *G. ahousahtiae* had homologs in the genome of

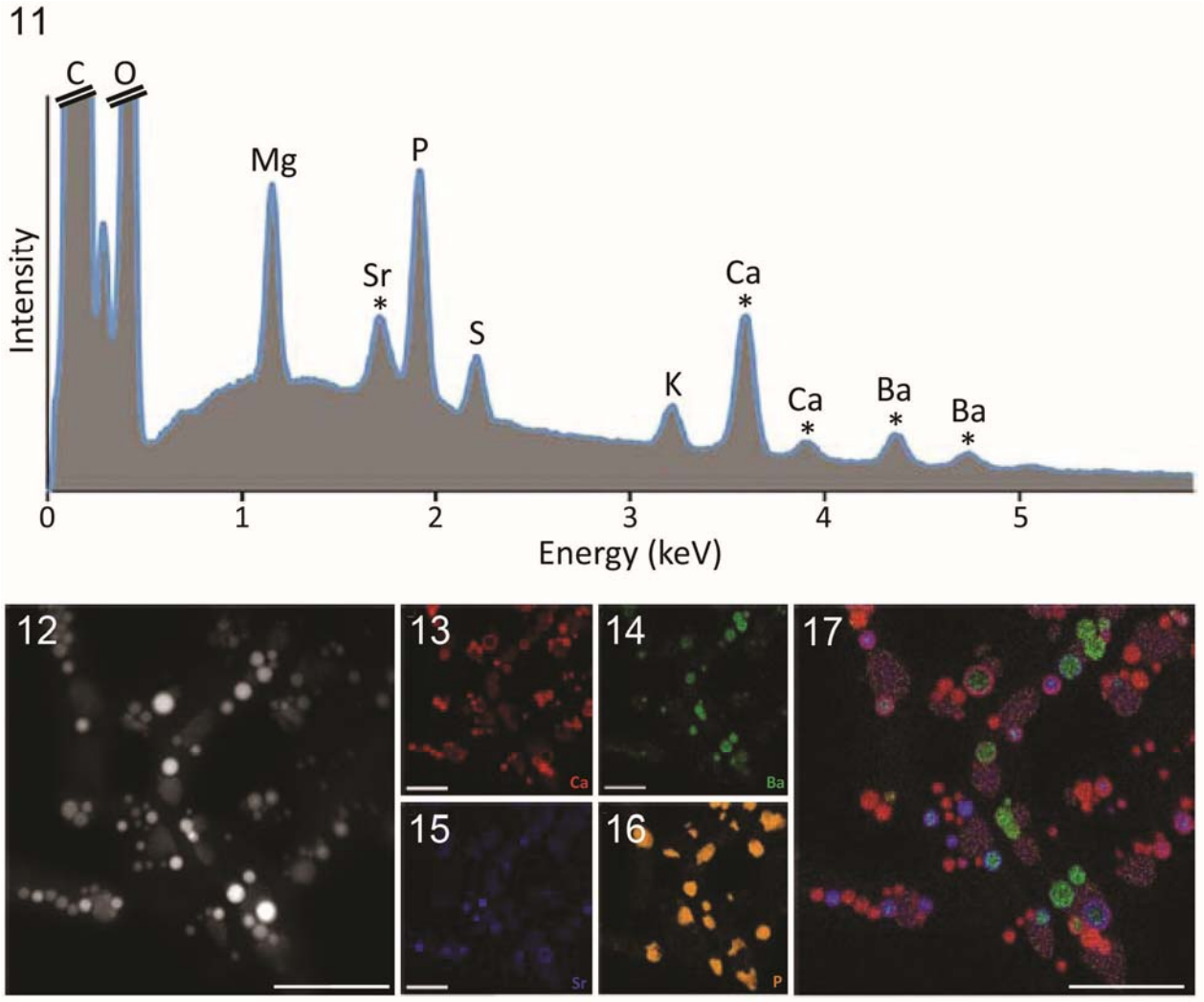


**Figs 11–17.** SEM-EDXS and STEM-EDXS analyses of *Gloeomargarita ahousahtiae* cells after one month of growth. **Fig. 11**. EDXS spectrum showing the presence of Ca, Ba and Sr in the cells. **Fig. 12**. STEM-HAADF image of cells showing carbonate (bright white) and polyphosphate (darker) inclusions. **Figs 13–16**. Ca (red), Ba (green), Sr (blue) and P (yellow) EDXS maps of these cells. **Fig. 17**. Overlay of the Ca, Ba, Sr and P EDXS maps. All scale bars correspond to 2 µm.

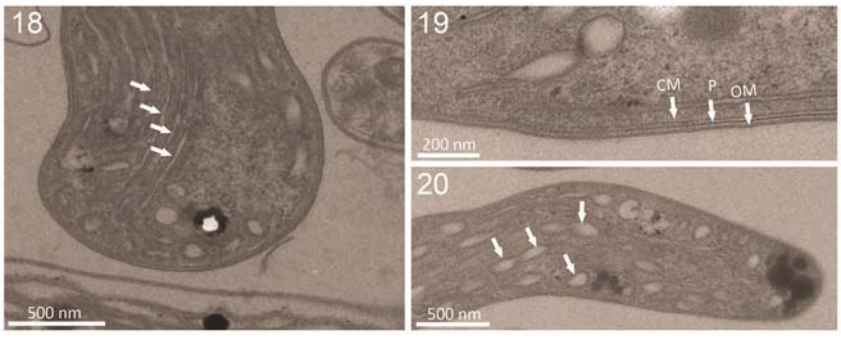


**Figs 18–20.** Transmission electron micrographs of thin sections of *Gloeomargarita ahousahtiae* cells. **Fig. 18**. Cell section showing thylakoids concentrated on one side of the cell (white arrows). **Fig. 19**. Cell section showing the cell (CM) and outer (OM) membranes and the peptidoglycan wall (P) between them. **Fig. 20**. Cell section showing numerous intracellular structures with low electron density (white arrows).

*G. lithophora*. We compared both Gloeomargaritales genomes using the average nucleotide identity (ANI) and the digital DNA-DNA hybridization (dDDH). We obtained values of 82.0% for the ANI and 24.90% for the dDDH, well below the thresholds (95% and 70%, respectively) commonly used to distinguish different species (Meier-Kolthoff *et al*., 2013; Rodríguez & Konstantinidis, 2014).

In addition to complete gene sets coding for the proteins involved in oxygenic photosynthesis and carbon fixation typical of cyanobacteria, the genome of *G. ahousahtiae* contains, among other important features, genes coding for a large set of nitrogenase

subunits (including *nifB, nifD, nifE, nifH, nifK, nifN, nifU, nifV, nifW, nifX* and *nifZ*) as well as a number of ABC transporters for metals and inorganic ions, such as bicarbonate, sulphate, nitrate, molybdate, iron, phosphate, manganese and cobalt.

### *Taxonomic analysis*

***Gloeomargarita ahousahtiae* T.Bacchetta, P.López-García, & D.Moreira, sp. nov.**

*Description*

Single-celled elongated rod-shaped cells with average cell size of 3.5–7.25 μm in length (average 5.1 μm) and 1.0–1.5 μm in width (average 1.2 μm). No mucilaginous sheath visible around the cells. Cell division by binary fission. Shows slow benthic growth on surfaces at temperatures ranging from 37–50°C, with an optimum at 45°C in liquid BG-11 medium (no growth observed on solid media). Oxygenic photoautotrophic metabolism. Contains chlorophyll *a*, phycocyanin and carotenoids, and possesses thylakoids mainly located along one side of the cell. Uses Ba, Sr and Ca to form intracellular carbonate spherical inclusions. Polyphosphate granules and carboxysomes also visible in the cytoplasm.

HOLOTYPE: (here designated): Metabolically inactive material from type culture CCAP 1437/1 fixed in 1.5% formaldehyde and deposited on a microscope glass slide (FIslAho-1, FCME). Fig. 2 illustrates the holotype.

TYPE CULTURE: Laboratorio de Algas Continentales. Ecología y Taxonomía, UNAM, Mexico (PMC 919.15); also deposited at the Scottish Association for Marine Science as CCAP 1437/1.

TYPE LOCALITY: Hot Springs Cove hydrothermal system, Vancouver Island, Canada (49°21′59.99″N, 126°15′27.00″W), microbial mats in a small stream.

ETYMOLOGY: *Gloeomargarita ahousahtiae* sp. nov. (ahou.sah'ti.ae. N.L. gen. n. ahousahtiae, of the Ahousaht people); referring to the origin of the strain in the region of Vancouver Island occupied by the Ahousaht population.

DNA SEQUENCES: Sequences were deposited in GenBank with accession numbers OL708428 (16S rRNA gene) and OV696605 (complete genome).

## Discussion

Despite their phylogenetic proximity (98% sequence identity for the 16S rRNA genes; Fig. 1), the two Gloeomargaritales species *G. lithophora* and *G. ahousahtiae* exhibit important differences that support their distinction as separate species. An evident difference is the much higher optimal growth temperature of *G. ahousahtiae* (45°C instead of 30°C for *G. lithophora*), which makes it the first isolated thermophilic representative of the Gloeomargaritales. The 16S rRNA gene sequence of *G. ahousahtiae* is closely related to several environmental sequences from continental hydrothermal systems (Fig. 1). Moderate thermophily seems to be the most widespread phenotype among the Gloeomargaritales, as deduced from the diversity of environmental sequences obtained from continental hot springs in various continents (see Fig. 1; Amarouche-Yala *et al*., 2014; Ragon *et al*., 2014). In that sense, *G. ahousahtiae* constitutes a good representative model to study the biology of this cyanobacterial order in relation to thermophily.

The two Gloeomargaritales species exhibit other significant differences. At the ultrastructural level, whereas *G. lithophora* has thylakoids arranged as concentric layers beneath the cytoplasmic membrane (Blondeau *et al*., 2018), those of *G. ahousahtiae* appear in most cells concentrated on one side of the cell (Fig. 18). Differences in thylakoid structure are common between mesophilic and thermophilic cyanobacteria, with a tendency to be more irregular in the latter (Mareš *et al*., 2019). Although recent studies indicate that thylakoid morphology has limited taxonomic value at large evolutionary scales (Mareš *et al*., 2019), it appears to be conserved at the genus level, making the difference between the two *Gloeomargarita* species unusual and a clear distinctive morphological character. From a metabolic point of view, *G. ahousahtiae* possesses a large set of *nif* genes comparable to that of non-heterocystous diazotrophic cyanobacteria (e.g. Nonaka *et al*., 2019) and that probably allows it to synthesize a functional nitrogenase complex. These genes are absent in *G. lithophora*. *Gloeomargarita ahousahtiae* also possesses genes coding for ABC transporters involved in bicarbonate, molybdate and cobalt uptake, which are also absent in *G. lithophora*.

Despite these differences, both *Gloeomargarita* species share the presence of numerous intracellular carbonate inclusions (Figs 7–10). Although this biomineralization process can be found in several other cyanobacterial groups (Benzerara *et al*., 2022), the two *Gloeomargarita* species are unique in their strong preference to use strontium and barium over calcium to synthesize their carbonate inclusions (Cam *et al*., 2016 and this work). Therefore, this seems to be a general trait in the *Gloeomargarita* species, common to both mesophilic and thermophilic strains, and constitutes a distinctive characteristic of this genus. The putative function of these intracellular carbonate granules remains unknown. One possibility is that they participate in the control of cell buoyancy by increasing the cell density, which might be especially relevant in benthic species such as the Gloeomargaritales. Alternatively, these inclusions might be a by-product of photosynthesis, which can increase intracellular pH and induce

carbonate precipitation in the presence of bivalent cations such as $Ca^{2+}$. However, this does not explain the marked preference of Gloeomargaritales to incorporate strontium and barium in their carbonates, which suggests the existence of an active mechanism to transport these elements (Cam *et al*., 2016; Benzerara *et al*., 2022). Further research is necessary to understand the possible role of these intracellular biominerals in cyanobacteria.


## Acknowledgements

We thank Prof. Denis Lynn for help with sampling; the UNICELL single-cell genomics platform (https://www.deemteam.fr/en/unicell) for Nanopore sequencing, and Prof. Michael Guiry for help with the taxonomic description. This work has benefited from the facilities and expertise of MIMA2 (Université Paris-Saclay, INRAE, AgroParisTech, 78350, Jouy-en-Josas, France) microscopy platform. We thank Vlad Costache (MIMA2 – Micalis Institute) for help with SEM imaging.

## Funding

This research was funded by the Agence Nationale de la Recherche project 'Microbialites' [No. ANR-18-CE02 -0013] and the European Research Council Advanced Grant 'Plast-Evol' [No. 787904].


## Supplementary information

The following supplementary material is accessible via the Supplementary Content tab on the article's online page at https://doi.org/10.1080/09670262.2023.2216257

**Supplementary fig. S1.** Laboratory aquaria incubated at 45°C showing the growth of a cyanobacterial biofilm. **Supplementary fig. S2.** Sampling site at Hot Springs Cove hydrothermal system showing conspicuous thermophilic microbial mats.

## Data availability

The 16S rRNA gene and complete genome sequences of *Gloeomargarita ahousahtiae* have been submitted to GenBank (accession numbers OL708428 and OV696605, respectively).

## Author contributions

T. Bacchetta: isolated the new strain, carried out molecular, phylogenetic and morphological analyses, and wrote the manuscript draft; P. López-García: participated in sampling, supervised and coordinated the work, and wrote the final version of the manuscript; A. Gutiérrez-Preciado : contributed to genome sequencing and analysis; N. Mehta: took microphotographs and described the chemistry of intracellular carbonate inclusions; F. Skouri-Panet: took microphotographs and described the chemistry of intracellular carbonate inclusions; K. Benzerara: took microphotographs and described the chemistry of intracellular carbonate inclusions; M. Ciobanu: contributed to genome sequencing and analysis; N. Yubuki: carried out TEM observations; R. Tavera: established the conditions for long-term culture maintenance; D. Moreira: participated in sampling, supervised and coordinated the work, and wrote the final version of the manuscript. All authors read and approved the final version of the manuscript.

## References


Altschul, S.F., Madden, T.L., Schaffer, A.A., Zhang, J., Zhang, Z., Miller, W. & Lipman, D.J. (1997). Gapped BLAST and PSI-BLAST: a new generation of protein database search programs. *Nucleic Acids Research*, **25** (17): 3389–3402. doi: 10.1093/nar/25.17.3389.

Amarouche-Yala, S., Benouadah, A., El Ouahab, B.A. & López-García, P. (2014). Morphological and phylogenetic diversity of thermophilic cyanobacteria in Algerian hot springs. *Extremophiles*, **18**(6): 1035–1047. doi: 10.1007/s00792-014-0680-7.

Benzerara, K., Duprat, E., Bitard-Feildel, T., Caumes, G., Cassier-Chauvat, C., Chauvat, F., Dezi, M., Diop, S.I., Gaschignard, G., Görgen, S., Gugger, M., López-García, P., Millet, M., Skouri-Panet, F., Moreira, D. & Callebaut, I. (2022). A new gene family diagnostic for intracellular biomineralization of amorphous Ca-carbonates by Cyanobacteria. *Genome Biololoy and Evolution*, **14**(3): evac026. doi: 10.1093/gbe/evac026.

Benzerara, K., Skouri-Panet, F., Li, J., Ferard, C., Gugger, M., Laurent, T., Couradeau, E., Ragon, M., Cosmidis, J., Menguy, N., Margaret-Oliver, I., Tavera, R. & López-García, P. (2014). Intracellular Ca-carbonate biomineralization is widespread in cyanobacteria. *Proceedings of the National Academy of Sciences*, **111**(30): 10933–10938. doi: 10.1073/pnas.1403510111.

Blank, C.E. (2013). Origin and early evolution of photosynthetic eukaryotes in freshwater environments: reinterpreting proterozoic paleobiology and biogeochemical processes in light of trait evolution. *Journal of Phycology*, **49**(6): 1040–1055. doi: 10.1111/jpy.12111.

Blondeau, M., Sachse, M., Boulogne, C., Gillet, C., Guigner, J.M., Skouri-Panet, F., Poinsot, M., Ferard, C., Miot, J. & Benzerara, K. (2018). Amorphous calcium carbonate granules form within an intracellular compartment in calcifying cyanobacteria. *Frontiers in Microbiology*, **9**: 1768. doi: 10.3389/fmicb.2018.01768.

Cam, N., Benzerara, K., Georgelin, T., Jaber, M., Lambert, J.F., Poinsot, M., Skouri-Panet, F. & Cordier, L. (2016). Selective uptake of alkaline earth metals by cyanobacteria forming intracellular carbonates. *Environmental Science & Technology*, **50**(21): 11654–11662. doi: 10.1021/acs.est.6b02872.

Cam, N., Benzerara, K., Georgelin, T., Jaber, M., Lambert, J. F., Poinsot, M., Skouri-Panet, F., Moreira, D., López-García, P., Raimbault, E., Cordier, L. & Jézéquel, D. (2017). Cyanobacterial formation of intracellular Ca-carbonates in undersaturated solutions. *Geobiology*, **16**(1): 49–61. doi: 10.1111/gbi.12261.

Capella-Gutiérrez, S., Silla-Martínez, J.M. & Gabaldón, T. (2009). trimAl: a tool for automated alignment trimming in large-scale phylogenetic analyses. *Bioinformatics*, **25** (15): 1972–1973. doi: 10.1093/bioinformatics/btp348.

Chen, M.Y., Teng, W.K., Zhao, L., Hu, C.X., Zhou, Y.K., Han, B.P., Song, L.R. & Shu, W.S. (2021). Comparative genomics reveals insights into cyanobacterial evolution

and habitat adaptation. *ISME Journal*, **15**(1): 211–227. doi: 10.1038/s41396-020-00775-z.

Couradeau, E., Benzerara, K., Gerard, E., Moreira, D., Bernard, S., Brown, G.E. & López-García, P. (2012). An early-branching microbialite cyanobacterium forms intracellular carbonates. *Science*, **336**(6080): 459–462. doi: 10.1126/science.1216171.

Dagan, T., Roettger, M., Stucken, K., Landan, G., Koch, R., Major, P., Gould, S.B., Goremykin, V.V., Rippka, R., Tandeau de Marsac, N., Gugger, M., Lockhart, P.J., Allen, J.F., Brune, I., Maus, I., Pühler, A. & Martin, W. F. (2013). Genomes of stigonematalean cyanobacteria (Subsection V) and the evolution of oxygenic photosynthesis from prokaryotes to plastids. *Genome Biology and Evolution*, **5**(1): 31–44. doi: 10.1093/gbe/evs117.

Hayat, M.A. (2000). *Principles and techniques of electron microscopy: biological applications*. Cambridge University Press, Cambridge.

Irisarri, I., Strassert, J.F.H. & Burki, F. (2021). Phylogenomic insights into the origin of primary plastids. *Systematic Biology*, **71**(1): 105–120. doi: 10.1093/sysbio/syab036.

Karnovsky, M. (1964). A formaldehyde-glutaraldehyde fixative of high osmolality for use in electron microscopy. *Journal of Cell Biology*, **27**: 1A–149A.

Katoh, K. & Standley, D.M. (2013). MAFFT multiple sequence alignment software version 7: improvements in performance and usability. *Molecular Biology and Evolution*, **30**(4): 772–780. doi: 10.1093/molbev/mst010.

Keeling, P.J. (2013). The number, speed, and impact of plastid endosymbioses in eukaryotic evolution. *Annual Review of Plant Biology*, **64**(1): 583–607. doi: 10.1146/annurev-arplant-050312-120144.

Mareš, J., Strunecký, O., Bučinská, L. & Wiedermannová, J. (2019). Evolutionary patterns of thylakoid architecture in cyanobacteria. *Frontiers in Microbiology*, **10**: 277. doi: 10.3389/fmicb.2019.00277.

McFadden, G.I. (2001). Primary and secondary endosymbiosis and the origin of plastids. *Journal of Phycology*, **37** (6): 951–959. doi: 10.1046/j.1529-8817.2001.01126.x.

McNeill, J., Barrie, F.R., Buck, W.R., Demoulin, V., Greuter, W., Hawksworth, D.L., Herendeen, P.S., Knapp, S., Marhold, K., Prado, J., Prud'homme van Reine, W.F., Smith, G.F., Wiersema, J.H. & Turland, J. (2012). *International code of nomenclature for algae, fungi, and plants (Melbourne code) regnum vegetabile*. Vol. **154**. Koeltz Scientific Books, Oberreifenberg, Germany.

Mehta, N., Bougoure, J., Kocar, B.D., Duprat, E. & Benzerara, K. (2022). Cyanobacteria accumulate radium (226 Ra) within intracellular amorphous calcium carbonate inclusions. *ACS EST Water*, **2**(4): 616–623. doi: 10. 1021/acsestwater.1c00473.

Meier-Kolthoff, J.P., Auch, A.F., Klenk, H.P. & Göker, M. (2013). Genome sequence-based species delimitation with confidence intervals and improved distance functions. *BMC Bioinformatics*, **14**(1): 60. doi: 10.1186/ 1471-2105-14-60.

Meier-Kolthoff, J.P., Carbasse, J.S., Peinado-Olarte, R.L. & Göker, M. (2021). TYGS and LPSN: a database tandem for fast and reliable genome-based classification and nomenclature of prokaryotes. *Nucleic Acids Research*, **50**(D1): D801–D807. doi: 10.1093/nar/ gkab902.

Moreira, D., Le Guyader, H. & Philippe, H. (2000). The origin of red algae and the evolution of chloroplasts. *Nature*, **405**(6782): 69–72. doi: 10.1038/35011054.

Moreira, D. & Philippe, H. (2001). Sure facts and open questions about the origin and evolution of photosynthetic plastids. *Research in Microbiology*, **152**(9): 771–780. doi: 10.1016/S0923-2508(01)01260-8.

Moreira, D., Tavera, R., Benzerara, K., Skouri-Panet, F., Couradeau, E., Gérard, E., Loussert-Fonta, C., Novelo, E., Zivanovic, Y. & López-García, P. (2018). Description of Gloeomargarita lithophora gen. nov., sp. nov., a thylakoid-bearing, basal-branching cyanobacterium with intracellular carbonates, and proposal for Gloeomargaritales ord. nov. *International Journal of Systematic and Evolutionary Microbiology*, **67**(3): 653–658. doi: 10.1099/ijsem.0.001679.

Nguyen, L.-T., Schmidt, H.A., von Haeseler, A. & Minh, B. Q. (2015). IQ-TREE: a fast and effective stochastic algorithm for estimating maximum-likelihood phylogenies. *Molecular Biology and Evolution*, **32**(1): 268–274. doi: 10. 1093/molbev/msu300.

Nonaka, A., Yamamoto, H., Kamiya, N., Kotani, H., Yamakawa, H., Tsujimoto, R. & Fujita, Y. (2019). Accessory proteins of the nitrogenase assembly, NifW, NifX/ NafY,and NifZ, are essential for diazotrophic growth in the nonheterocystous cyanobacterium. *Leptolyngbya Boryana. Frontiers in Microbiology*, **10**: 495. doi: 10.3389/fmicb.2019.00495.

Ponce-Toledo, R.I., Deschamps, P., López-García, P., Zivanovic, Y., Benzerara, K. & Moreira, D. (2017). An early-branching freshwater cyanobacterium at the origin of plastids. *Current Biology*, **27**(3): 386–391. doi: 10. 1016/j.cub.2016.11.056.

Ponce-Toledo, R.I., López-García, P. & Moreira, D. (2019). Horizontal and endosymbiotic gene transfer in early plastid evolution. *New Phytologist*, **224**(2): 618–624. doi: 10.1111/nph.15965.

Ragogn, M., Benzerara, K., Moreira, D., Tavera, R. & López-García, P. (2014). 16S rDNA-based analysis reveals cosmopolitan occurrence but limited diversity of two cyanobacterial lineages with contrasted patterns of intracellular carbonate mineralization. *Frontiers in Microbiology*, **5**: 1–11. doi: 10.3389/fmicb.2014.00331.

Riding, R. (2006). Cyanobacterial calcification, carbon dioxide concentrating mechanisms, and proterozoic-cambrian changes in atmospheric composition. *Geobiology*, **4**(4): 299–316. doi: 10.1111/j.1472-4669.2006.00087.x.

Rodríguez-Ezpeleta, N., Brinkmann, H., Burey, S.C., Roure, B., Burger, G., Löffelhardt, W., Bohnert, H.J., Philippe, H. & Lang, B.F. (2005). Monophyly of primary photosynthetic eukaryotes: green plants, red algae, and glaucophytes. *Current Biology*, **15**(14): 1325–1330. doi: 10.1016/j.cub.2005.06.040.

Rodríguez, L.M. & Konstantinidis, K.T. (2014). Bypassing cultivation to identify bacterial species: culture-independent genomic approaches identify credibly distinct clusters, avoid cultivation bias, and provide true insights into microbial species. *Microbe*, **9**: 111–118.

Seemann, T. (2014). Prokka: rapid prokaryotic genome annotation. *Bioinformatics*, **30**(14): 2068–2069. doi: 10. 1093/bioinformatics/btu153.

Stanier, R.Y., Kunisawa, R., Mandel, M. & Cohen-Bazire, G. (1971). Purification and properties of unicellular blue–green algae (Order chroococcales). *Bacteriological Reviews*, **35**(2): 171–205. doi: 10.1128/br.35.2.171-205.1971.

Wick, R.R., Judd, L.M., Gorrie, C.L. & Holt, K.E. (2017). Unicycler: resolving bacterial genome assemblies from short and long sequencing reads. *PLoS Computational*

*Biology*, **13**(6): e1005595. doi: 10.1371/journal.pcbi.1005595.

Yoon, S.H., Ha, S., Lim, J., Kwon, S. & Chun, J. (2017). A large-scale evaluation of algorithms to calculate average nucleotide identity. *Antonie van Leeuwenhoek*, **110**(10): 1281–1286. doi: 10.1007/s10482-017-0844-4.